Supporting Information

Visible-Light Photooxidation in Water by $^1O_2$-Generating Supramolecular Hydrogels

Sankarsan Biswas,[a,b,c] Mohit Kumar,[a,b] Andrew M. Levine,[a,b,c] Ian Jimenez,[a,e] Rein V. Ulijn,* [a,b,c,d] Adam B. Braunschweig* [a,b,c,d]

[a] Advanced Science Research Center, City University of New York, 85 St. Nicholas Terrace, New York, NY 10031, USA

[b] Department of Chemistry, Hunter College, 695 Park Avenue, New York, NY 10065, USA

[c] PhD Program in Chemistry, Graduate Center, City University of New York, 365 5th Avenue, New York, NY 10016, USA

[d] PhD Program in Biochemistry, Graduate Center, City University of New York, 365 5th Avenue, New York, NY 10016, USA

[e] The High School for Math, Science, and Engineering, The City College of New York, 240 Convent Avenue New York, NY 10031, USA

*Corresponding Author: abraunschweig@gc.cuny.edu

rulijn@gc.cuny.edu

Table of Contents

1. Organic Synthesis

All reagents and starting materials were purchased from Aldrich or VWR and used without further purification unless otherwise noted. Thin-layer chromatography was carried out using aluminum sheets precoated with silica gel 60 (EMD 40 - 60 mm, 230 - 400 mesh with 254 nm dye). Silica gel (BDH 60Å) was used for flash column chromatography. All solvents were dried prior to use, and all reactions were carried out under Ar atmosphere using standard Schlenk techniques. Deuterated solvents were purchased from Cambridge Isotope Laboratories Inc. and used as received. NMR spectra were obtained on a Bruker 300 MHz spectrometer. All chemical shifts were reported in ppm units (δ) using residual solvent as the internal reference. Electrospray ionization mass spectra were acquired on an Agilent LC/MSD Trap XCT system. High-resolution Mass spectra analyses were carried out on an Agilent 6200 LC/MSD TOF system.

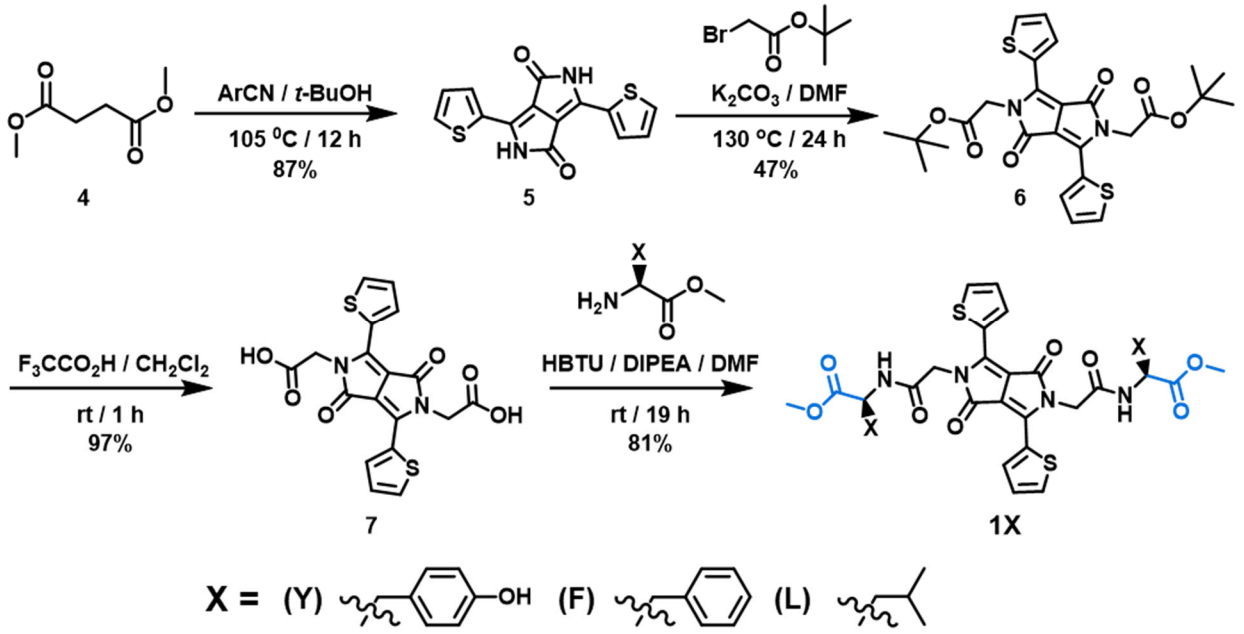

Scheme S1: Synthesis of DPP-$(XOMe)_2$ (**1X, X = Y, F, L**)

Synthesis of 5: 5 was synthesized following a previously reported literature procedure and its characterization data were in good agreement with the reported data.[1]

Synthesis of 6: To a solution of **3** (1.0 g, 3.3 mmol) in dry DMF (15 mL), *tert*-butyl bromoacetate (1.5 mL, 9.9 mmol) and K_2CO_3 was added (1.9 g, 14 mmol) and the mixture was heated at 130 ^{0}C for 24 h under positive Ar pressure. After 24 h TLC (1:1 EtOAc/n-hexane) indicated the absence of starting material. The reaction was cooled to ambient temperature. DMF was removed in vacuo at 80 ^{o}C and the remaining oil was redissolved in CH_2Cl_2 (100 mL). The solution was washed in a separatory funnel with H_2O (100 mL). The organic layer was collected and the aqueous phase was washed one more time with 100 mL CH_2Cl_2. All organic layers were combined, dried with $MgSO_4$, and solvent was removed under reduced pressure. The product was then purified by column chromatography (SiO_2 1:99 EtOAc:CH_2Cl_2) to provide a red solid (0.82 g, 47%). NMR data matched with the reported compound [1] that was prepared following a different route.

Synthesis of 7: 7 was synthesized following a previously reported literature procedure its characterization data were in good agreement with the reported data.[1]

Synthesis of DPP-(YOMe)$_2$ (1Y): 7 (1.0 g, 2.4 mmol), L-tyrosine methyl ester (1.3 g, 6.0 mmol), and HBTU (2.2 g, 5.8 mmol) were dissolved in dry DMF (29 mL) and stirred for 5 min under Ar. 2 mL DIPEA was then added to the reaction mixture and it was stirred under Ar for 22 h. DMF was removed under reduced pressure at 80 °C. 100 mL CH_2Cl_2 was then added to the reaction mixture and transferred into 400 mL H_2O. The resulting red solid was filtered, the solid was then stirred in 300 mL $NaHCO_3$ followed by 300 mL 1N HCl and finally with 300 mL water for 20 min each. Finally the solid was dried for 8h under high vacuo providing a red solid (1.5 g, 81%). ^{1}H NMR (300 MHz, DMSO-d6, 25 °C) δ 9.33 (s, 2H), 8.85 (d, J = 7.9 Hz, 2H), 8.53 (d, J = 3.9 Hz, 2H), 7.96 (d, J = 5.0 Hz, 2H), 7.40 – 7.28 (m, 2H), 7.04 (d, J = 8.3 Hz, 4H), 6.70 (d, J = 8.2 Hz, 4H), 4.65 (dd, J = 56.6, 18.1 Hz, 4H), 4.46 (dd, J = 13.7, 8.9 Hz, 2H), 3.62 (s, 3H), 3.04 – 2.91 (m, 2H), 2.83-2.75 (m, 2H). ^{13}C NMR (75 MHz, DMSO-d6, 25 °C) δ 172.30, 167.17, 160.71, 156.48, 140.23, 134.29, 132.99, 130.64, 130.01, 128.94, 127.53, 115.62, 106.63, 54.41, 52.41, 44.43, 36.56. HRMS m/z calculated for $C_{38}H_{34}N_4O_{10}S_2$ [(M+H)$^+$] 771.1789, found 771.1785.

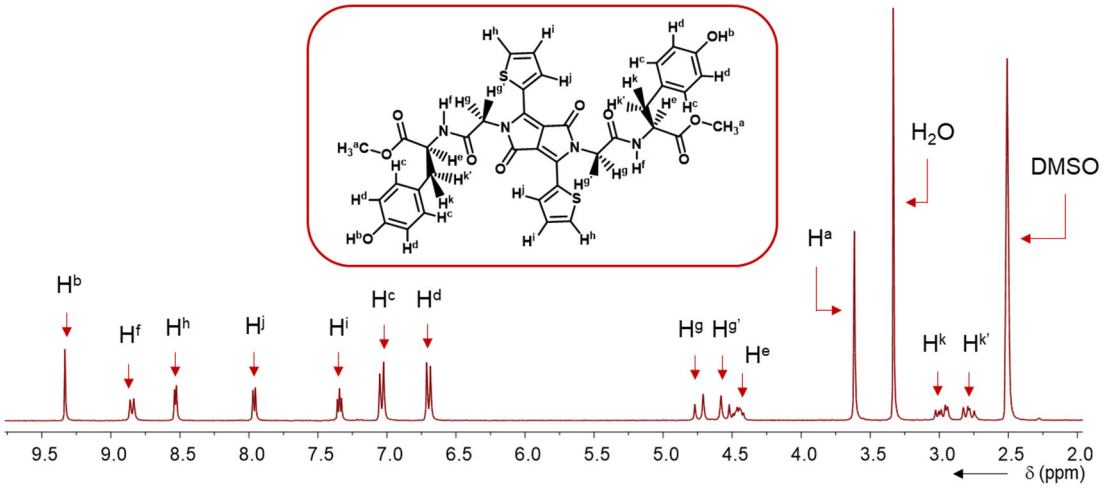

Figure S1. ^{1}H NMR of DPP-(YOMe)$_2$ (**1Y**) (300 MHz, 25 °C) in DMSO-d6.

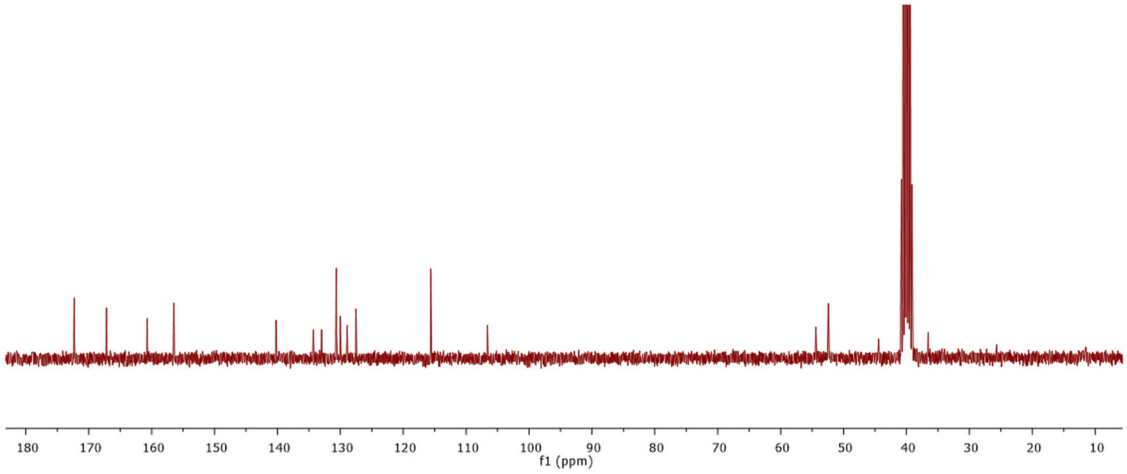

Figure S2. ^{13}C NMR of DPP-(YOMe)$_2$ (**1Y**) (300 MHz, 25 °C) in DMSO-d6.

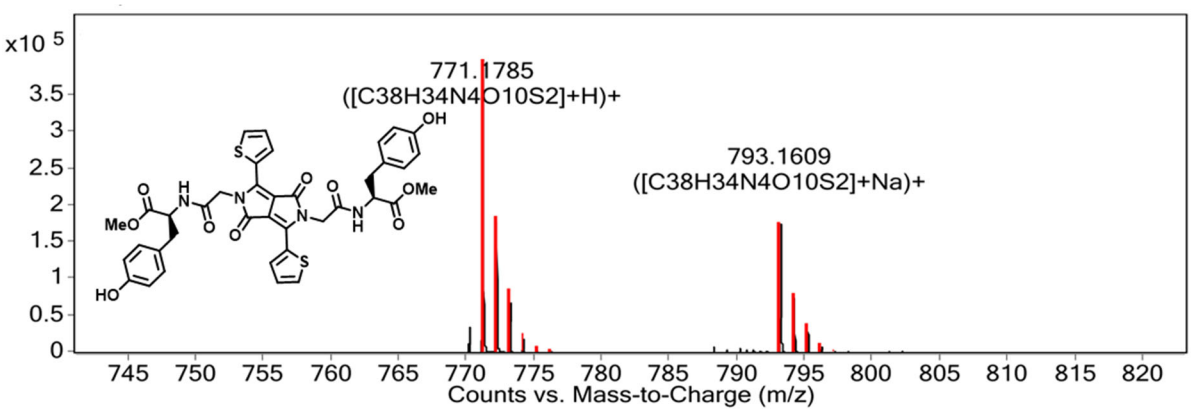

Figure S3. ESI HRMS spectrum of DPP-$(YOMe)_2$ (**1Y**).

Synthesis of DPP-$(FOMe)_2$ (1F): 4 (0.10 g, 2.4 mmol), L-phenylalanine methyl ester (1.3 g, 6.0 mmol) and HBTU (0.22 g, 5.8 mmol) were dissolved in dry DMF (3 mL) and stirred for 5 min under Ar. 0.2 mL DIPEA was then added to the reaction mixture and it was stirred under Ar for 22 h. DMF was then evaporated under reduced pressure at 80 °C. 5 mL CH_2Cl_2 was then added to transfer the reaction mixture into 200 mL Et_2O, and the solid was filtered and washed with 50 mL H_2O. This solid was again dissolved in 5 mL CH_2Cl_2 and precipitated again into Et_2O. This red solid was then washed with washed with 50 mL water for 20 min. Finally the solid was dried 8 h under high vacuum providing a red solid (0.18 g, 84%). ^{1}H NMR (300 MHz, $CDCl_3$, 25 °C) δ 8.60 (d, J = 3.2 Hz, 2H), 7.70 (d, J = 4.9 Hz, 2H), 7.32-7.30 (m, 2H), 7.19-7.09 (m, 10H), 6.59 (d, J = 7.4 Hz, 2H), 4.91 (dd, J = 13.8, 5.9 Hz, 2H), 4.73 (d, J = 3.0 Hz, 4H), 3.71 (s, 6H), 3.20-3.05 (m, 4H). ^{13}C NMR (75 MHz, $CDCl_3$, 25 °C) δ 171.39, 166.98, 161.26, 140.11, 135.39, 134.80, 131.92, 129.32, 129.15, 128.92, 128.59, 127.15, 107.36, 53.21, 52.44, 45.89, 37.75. HRMS m/z calculated for $C_{38}H_{34}N_4O_8S_2$ [$(M+H)^+$] 739.1891, found 739.1885

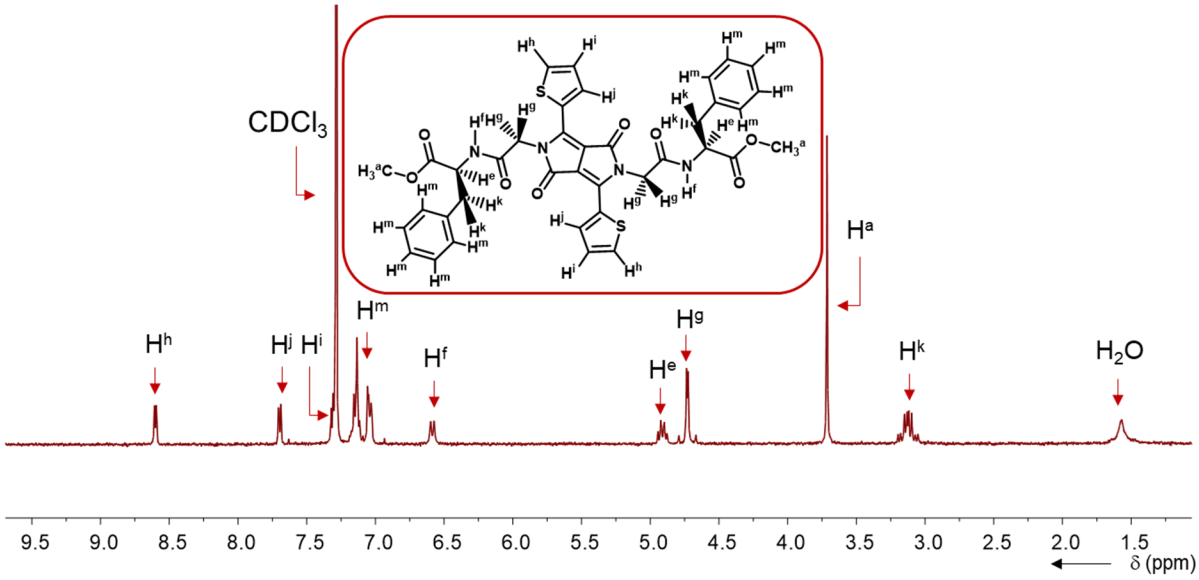

Figure S4. ^{1}H NMR of DPP-$(FOMe)_2$ (**1F**) (300 MHz, 25 °C) in $CDCl_3$.

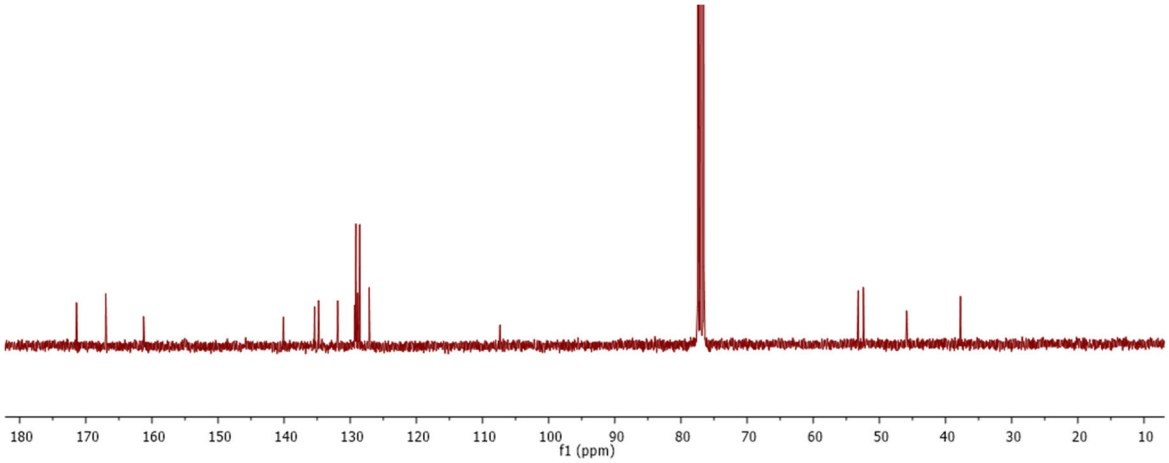

Figure S5. ^{13}C NMR of DPP-$(FOMe)_2$ (**1F**) (300 MHz, 25 °C) in $CDCl_3$.

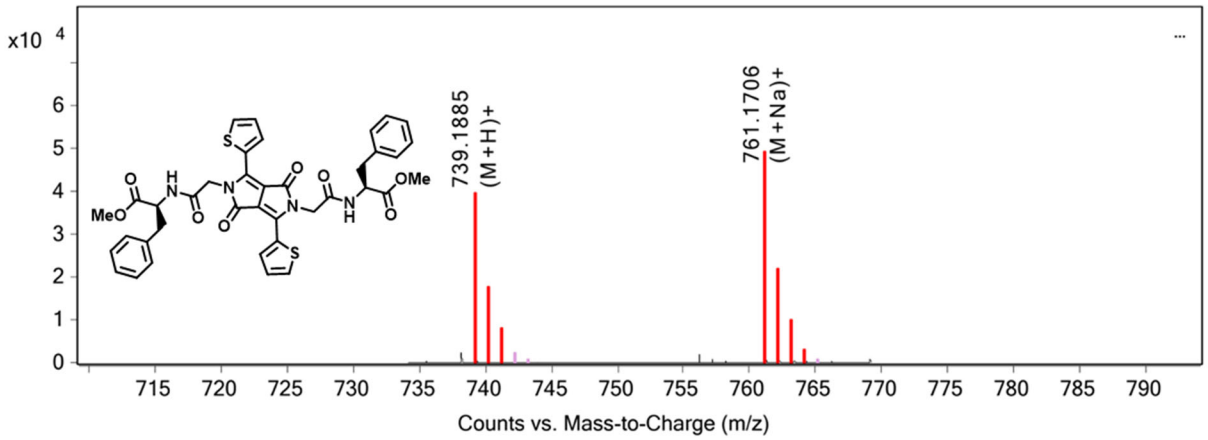

Figure S6. ESI HRMS spectra of DPP-$(FOMe)_2$ (**1F**).

DPP-$(LOMe)_2$ (1L): 4 (0.10 g, 2.4 mmol), L-leucine (1.3 g, 6.0 mmol) and HBTU (0.22 g, 5.8 mmol) were dissolved in dry DMF (3 mL) and stirred for 5 min under Ar. 0.2 mL DIPEA was then added to the reaction mixture and stirred under Ar for 22 h. DMF was then evaporated under reduced pressure at 80 °C. 5 mL CH_2Cl_2 was then added to reaction mixture, and the solution was transferred into 200 mL Et_2O. The red solid was then filtered and washed with 50 mL water. This solid was again dissolved in 5 mL CH_2Cl_2 and precipitated one more time in Et_2O. Finally, the red crystals were dried 8h under high vacuum (0.13 g, 81%). ^1H NMR (300 MHz, $CDCl_3$, 25 °C) δ 8.65 (dd, J = 3.9, 1.1 Hz, 2H), 7.69 (dd, J = 5.0, 1.1 Hz, 2H), 7.32 – 7.29 (m, 2H), 6.52 (d, J = 8.2 Hz, 2H), 4.78 (d, J = 1.9 Hz, 4H), 4.74 – 4.63 (m, 2H), 3.71 (s, 6H), 1.71 – 1.52 (m, 6H), 0.91 (d, J = 5.3 Hz, 12H). ^{13}C NMR (75 MHz, DMSO) δ 173.10, 167.34, 160.87, 140.21, 134.17, 133.13, 129.97, 129.01, 106.95, 52.39, 50.84, 44.49, 24.65, 23.27, 21.58. HRMS m/z calculated for $C_{32}H_{38}N_4O_8S_2$ [$(M+H)^+$] 671.2204, found 671.2205.

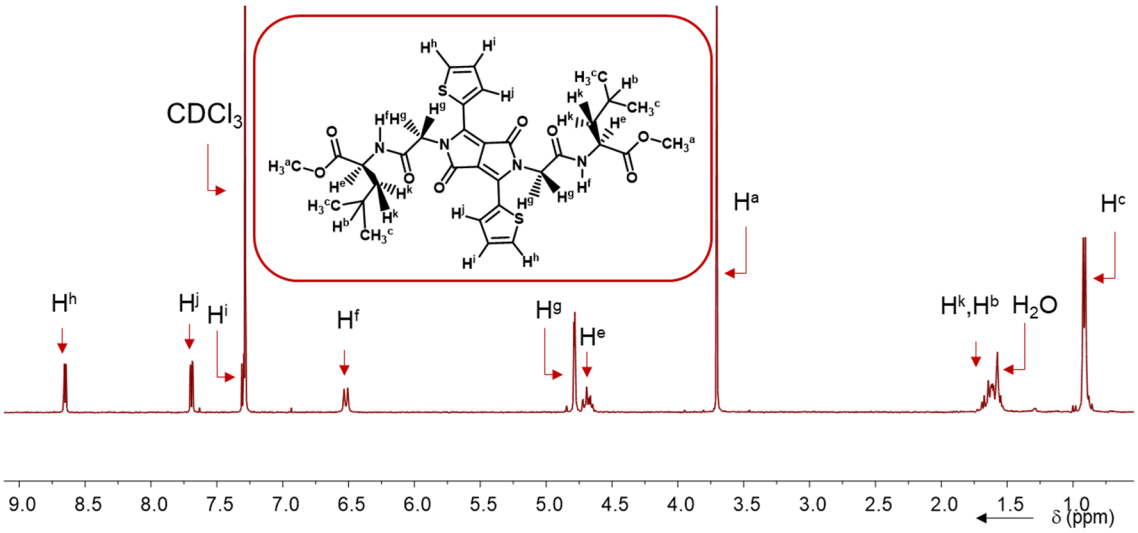

Figure S7. ^{1}H NMR of DPP-(LOMe)$_2$ (**1L**) (300 MHz, 25 °C) in $CDCl_3$.

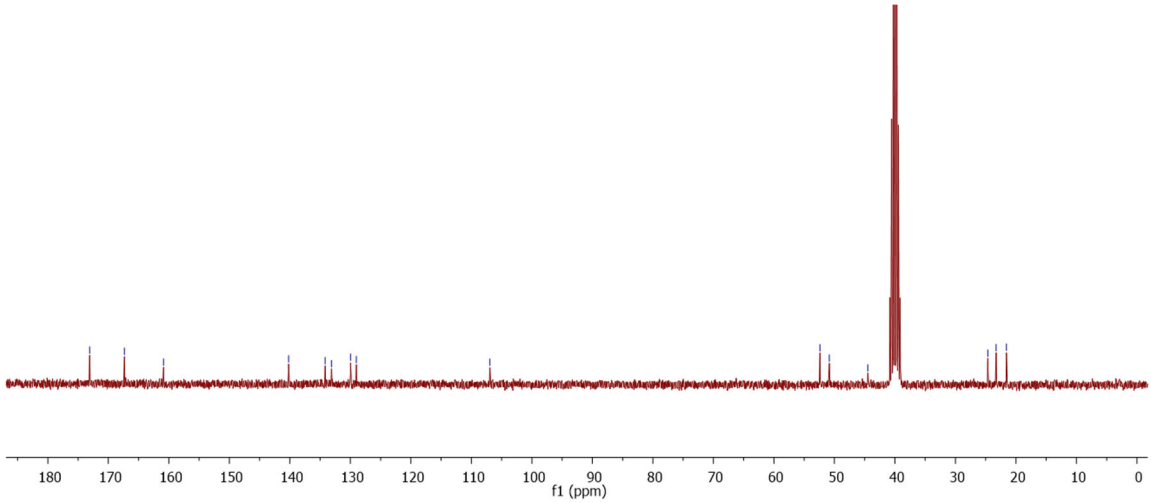

Figure S8. ^{13}C NMR of DPP-(LOMe)$_2$ (**1L**) (300 MHz, 25 °C) in DMSO-d6.

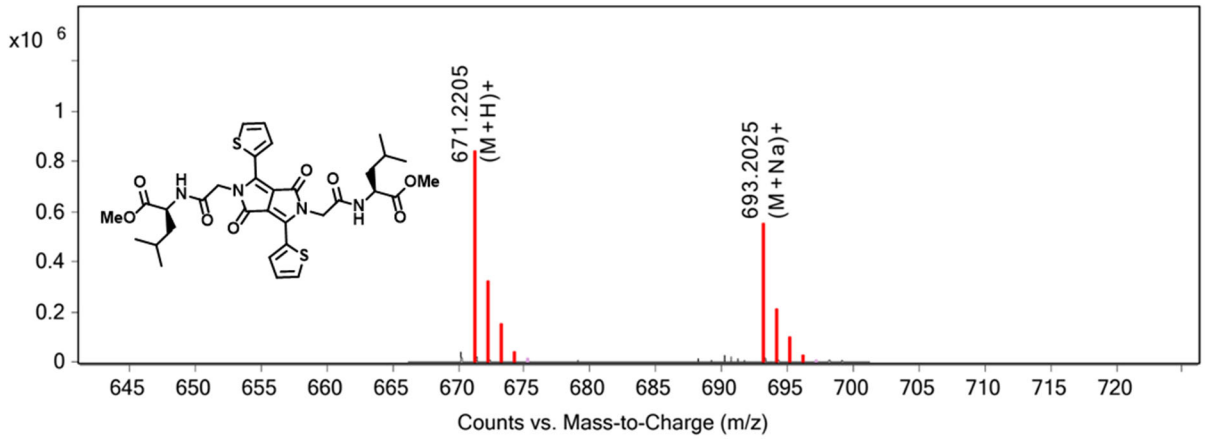

Figure S9. ESI HRMS spectrum of DPP-(LOMe)$_2$ (**1L**).

2. Gel Preparation

For the preparation of all gels studied herein, we used the following procedure. A stock solution of DPP-$(XOMe)_2$ was prepared in DMSO (200 mM). The desired concentrations of all samples were obtained by diluting this solution with 100 mM phosphate buffer (pH 8) and 1 mg ml^{-1} of α-chymotrypsin. The vial containing enzyme in phosphate buffer was sonicated while the required amount of DMSO stock solution of DPP-$(XOMe)_2$ was added into the sample and sonicated for 30 s after addition. After 1 h this reaction mixture was then vortexed and sonicated for 30 s to obtain the gel. In the case of DPP-$(FOMe)_2$, the solid was directly weighed in a vial with different amounts depending upon the desired final concentrations and then DMSO was added. This solution was then heated to dissolve DPP-$(FOMe)_2$ completely and phosphate buffer was added to this hot solution to dilute DMSO to 10%. Enzyme solution was then added into this mixture after the mixture cooled to rt, and sonicated and vortexed for 60 s. After 1 h this reaction mixture was then again vortexed and sonicated for 30 s to obtain the gel.

3. Atomic Force Microscopy

Samples were prepared by drop casting 5 µl of DPP-$(YOH)_2$ (10 mM in 100 mM phosphate buffer) onto freshly cleaved mica surfaces (G250–2 Mica sheets 1″ × 1 ″ × 0.006″ Agar Scientific Ltd) followed by blotting with filter paper. Then the surface was washed with 5 µl of deionized H_2O and blotted again to remove excess buffer salt. The surface was completely dried on bench top for 2 days before taking images. The images were obtained by scanning the mica surface under ambient conditions using a FastScan Microscope (Bruker) operated in ScanAsyst noncontact mode. The AFM scans were taken at a resolution of 512 × 512 pixels. The images were analyzed using NanoScope Analysis software Version 1.40.

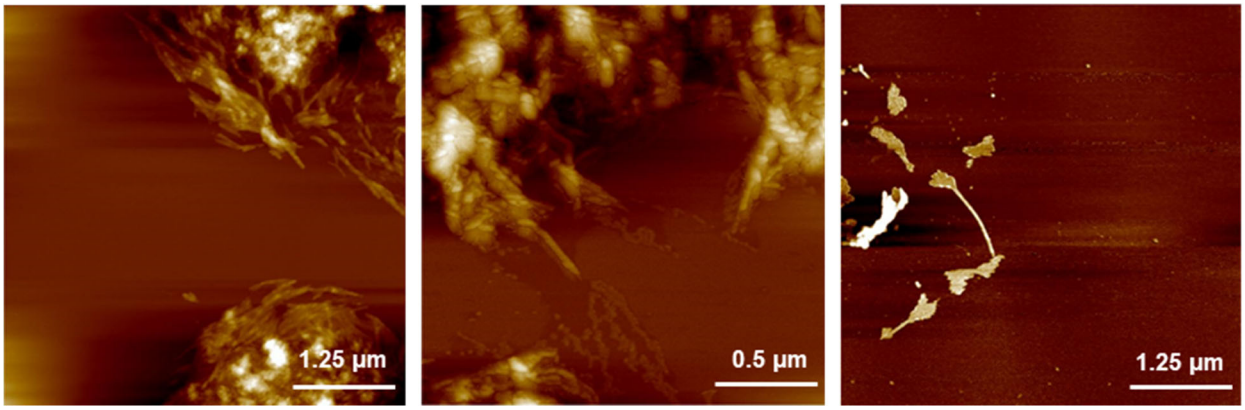

Figure S10. AFM height images of DPP-$(YOMe)_2$ (**1Y**).

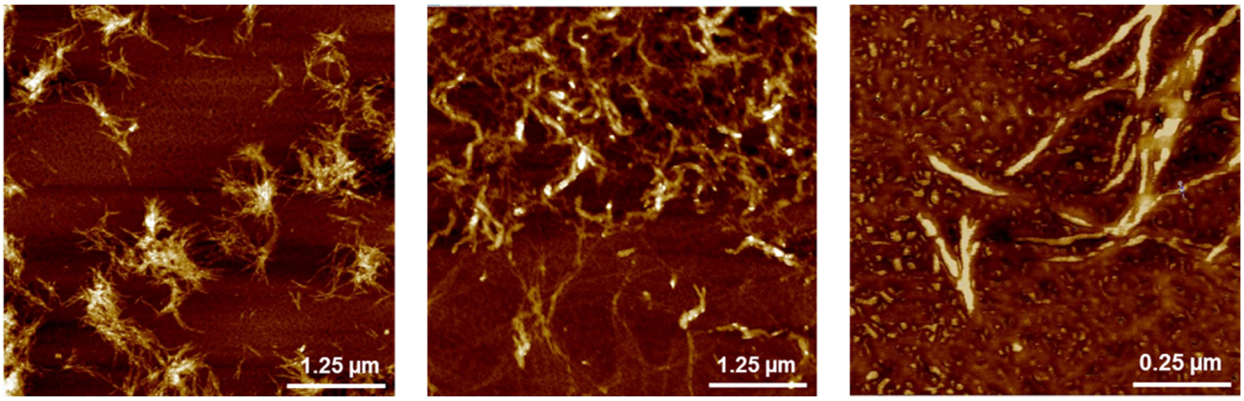

Figure S11. AFM height images of DPP-$(YOH)_2$ (**3Y**).

4. Transmission Electron Microscopy

All samples were prepared by drop casting 5 µL of DPP-$(XOH)_2$ (10 mM in 100 mM phosphate buffer) onto continuous carbon grids [Electron Microscope Sciences CF400-CU]. The solutions were allowed to sit on the grids for 30 s and then wicked dry from the grid edge using filter paper [Whatman Cat No. 1001-070]. Negative stain (5 µl of 1% aqueous methylamine vanadate (NanoVan; Nanoprobes)) was then applied and blotted again with filter paper [Whatman Cat No. 1001-070] to remove the excess. Stained samples were imaged using a 200 KeV FEI Titan Themis 200 transmission electron microscope equipped with an FEI Ceta 4k by 4k camera. The images were analyzed using ImageJ software.

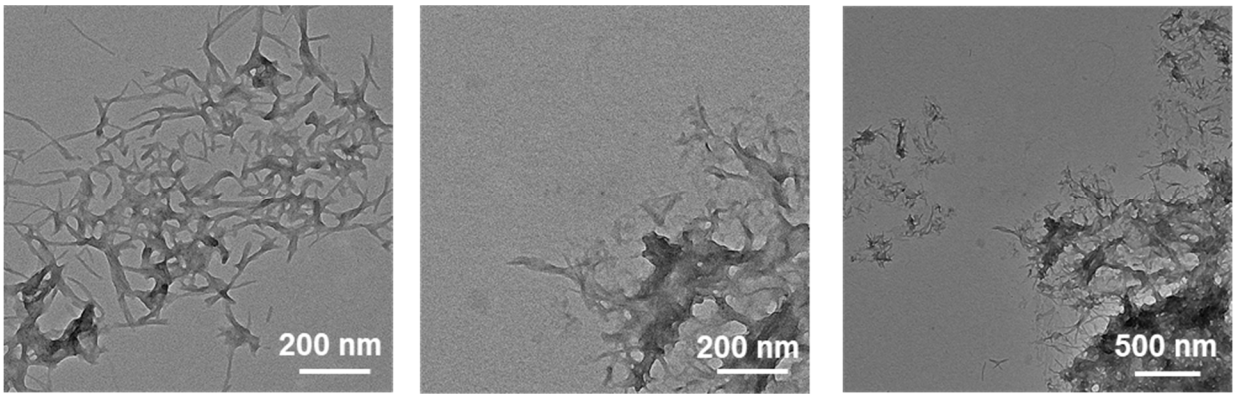

Figure S12. TEM images of DPP-$(YOMe)_2$ (**1Y**).

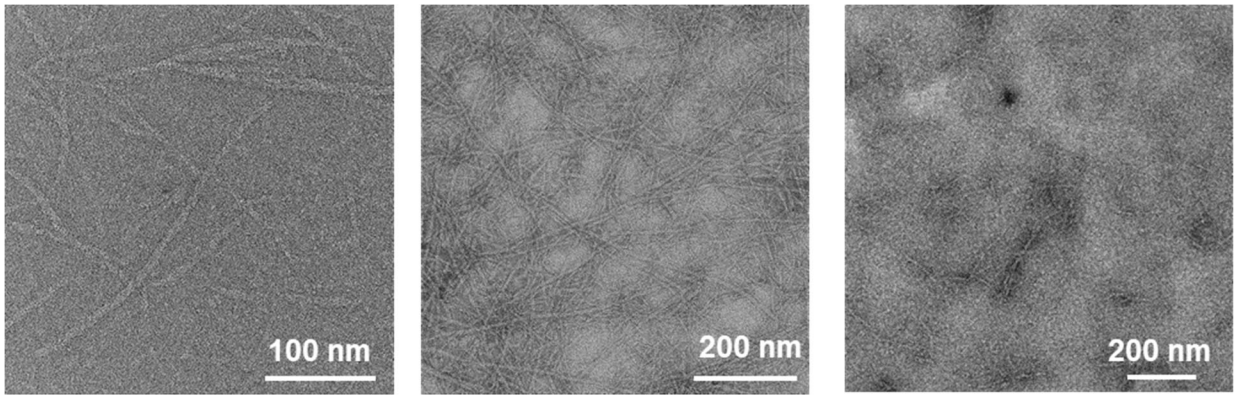

Figure S13. TEM images of DPP-$(YOH)_2$ (**3Y**).

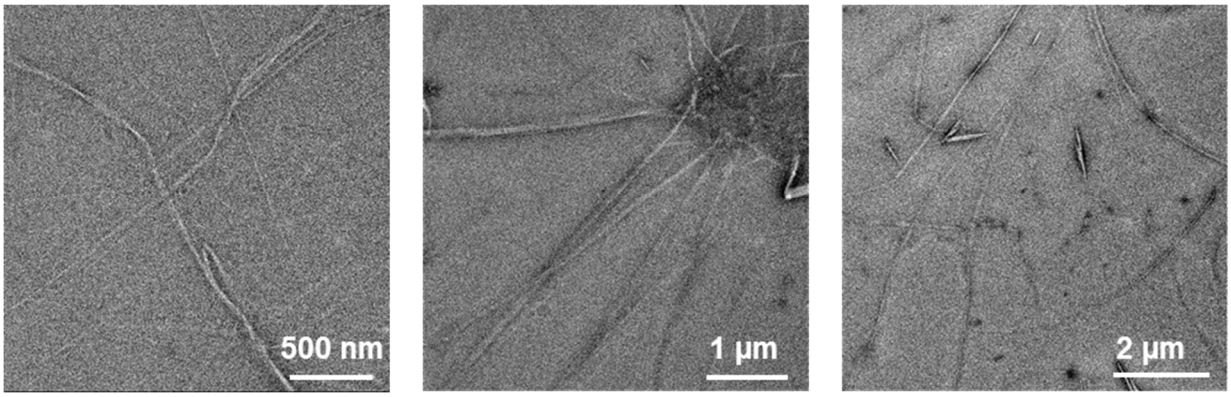

Figure S14. TEM images of DPP-$(LOH)_2$ (**3L**).

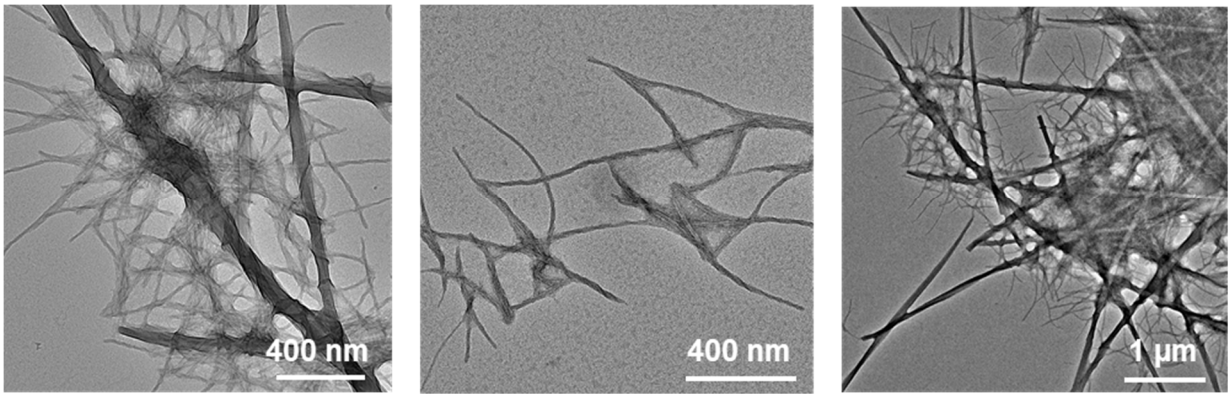

Figure S15. TEM images of DPP-$(FOH)_2$ (**3F**).

5. HPLC Analysis of the Hydrolysis of DPP-$(XOMe)_2$.

A Dionex P780 HPLC system equipped with a Macherey Nagel C18 column (250 mm length, 4.6 mm internal diameter and 3 µm particle size) was used to quantify the kinetics of enzyme-catalyzed conversions of DPP-$(XOMe)_2$ to DPP-$(ROH)_2$. For the HPLC sample, 10 µl of the reaction mixtures at different time points were diluted to 0.5 ml of with MeCN:H_2O (50:50). The eluting solvent system (all solvent contained 0.1% trifluoroacetic acid; flow rate 1 ml min^{-1}) had a linear gradient of 10% (v/v) MeCN in H_2O for 2 min, which gradually increased to 70% (v/v) MeCN in H_2O at 10 min and was kept constant until 12 min. Chromatograms were monitored at 520 nm and the relative areas under the peaks were used to identify the percentage product conversion. All chromatograms were normalized with respect to the total area to allow for direct comparison.

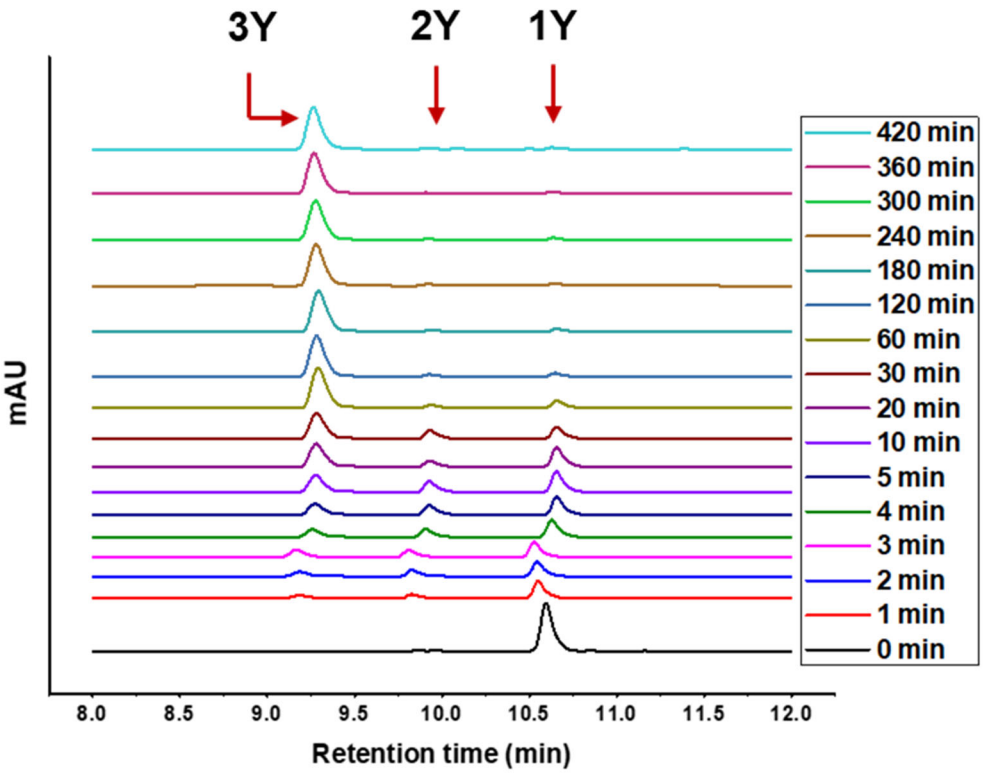

Figure S16. HPLC data for the conversion of **1Y** to **3Y**.

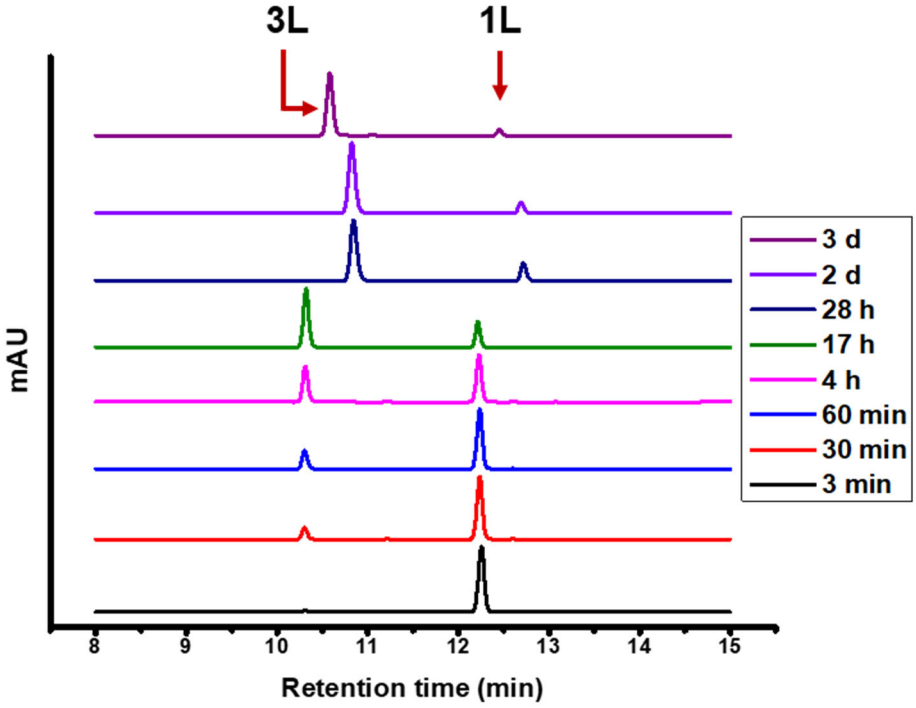

Figure S17. HPLC data for the conversion of **1L** to **3L**.

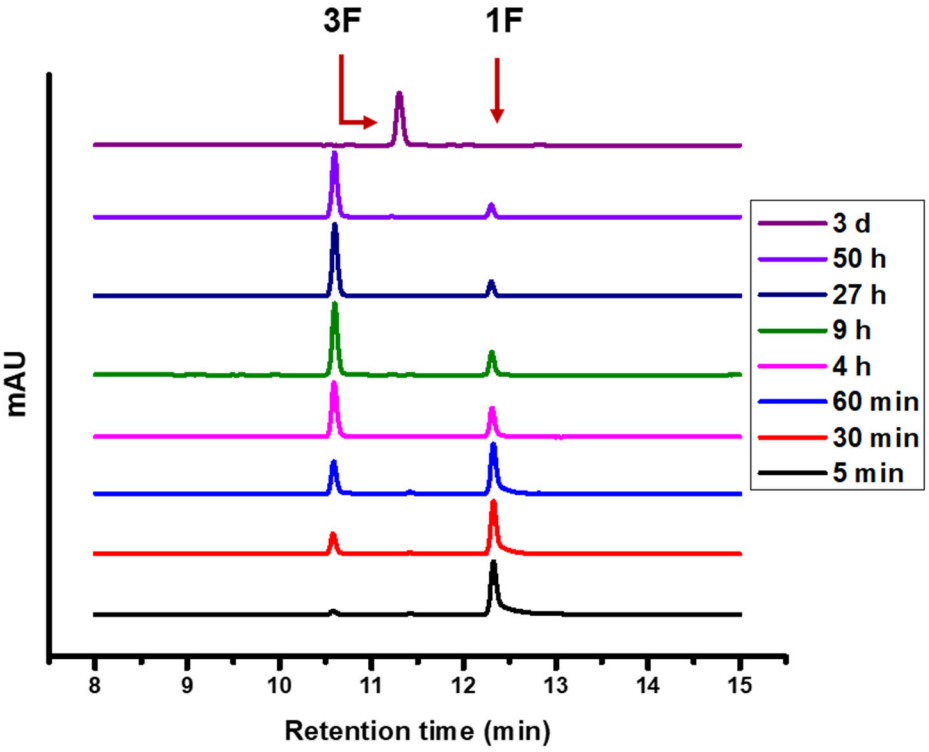

Figure S18. HPLC data for the conversion of **1F** to **3F**.

6. Circular dichroism of DPP-$(XOH)_2$

30 µl of reaction mixtures for the conversion of DPP-$(XOMe)_2$ to DPP-$(ROH)_2$ (10 mM in 100 mM phosphate buffer with 1 mg mL^{-1} α-chymotrypsin) at different time points were pipetted into a 0.1 mm demountable Hellma Analytics Art. No. 106-0.10-40 quartz cuvette, and the spectra were measured on a JASCO J-1500 spectrometer. The temperature was maintained at 20 °C for all the measurements.

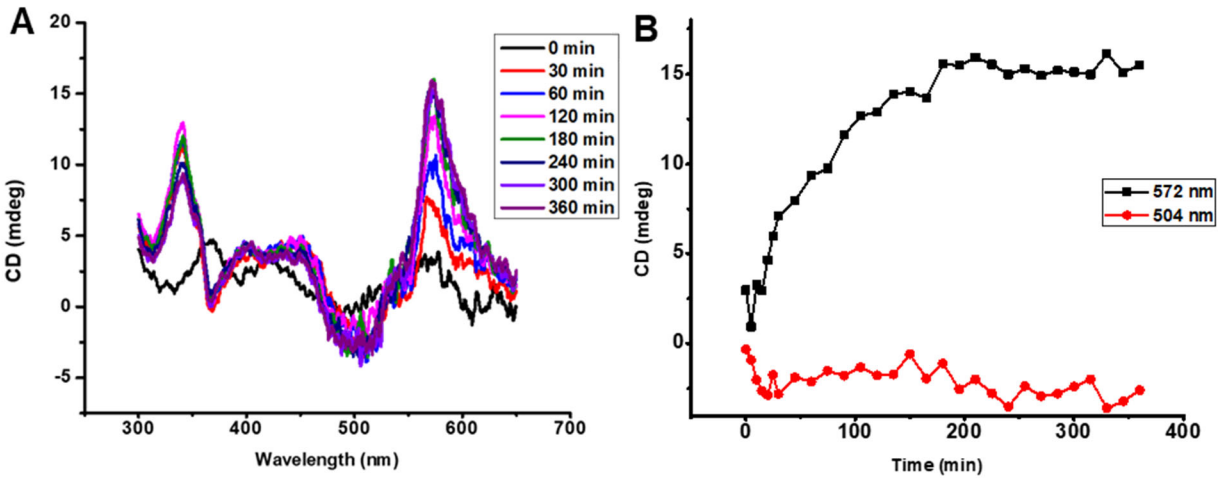

Figure S19. A) Formation for homochiral superstructure during *in situ* enzymatic hydrolysis of **1Y** monitored by CD. B) Tracking of CD signal at 572 nm and 504 nm.

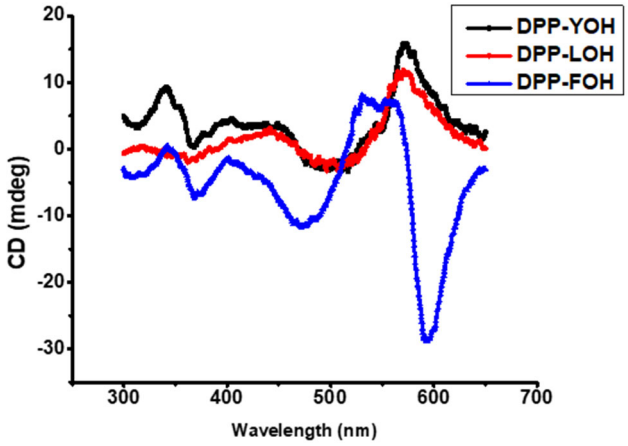

Figure S20. A) CD spectra of **3Y**, **3L** and **3F** at 10 mM.

7. UV-VIS spectroscopy

30 µl of reaction mixtures for the conversion of DPP-$(XOMe)_2$ to DPP-$(ROH)_2$ (10 mM in 100 mM phosphate buffer with 1 mg mL^{-1} α-chymotrypsin) at different time points were pipetted into a 0.1 mm demountable quartz cuvette and spectra were measured on a Jasco V-660 spectrophotometer at a scanning speed of 200 nm min^{-1}. Measurements were collected between 250-900 nm.

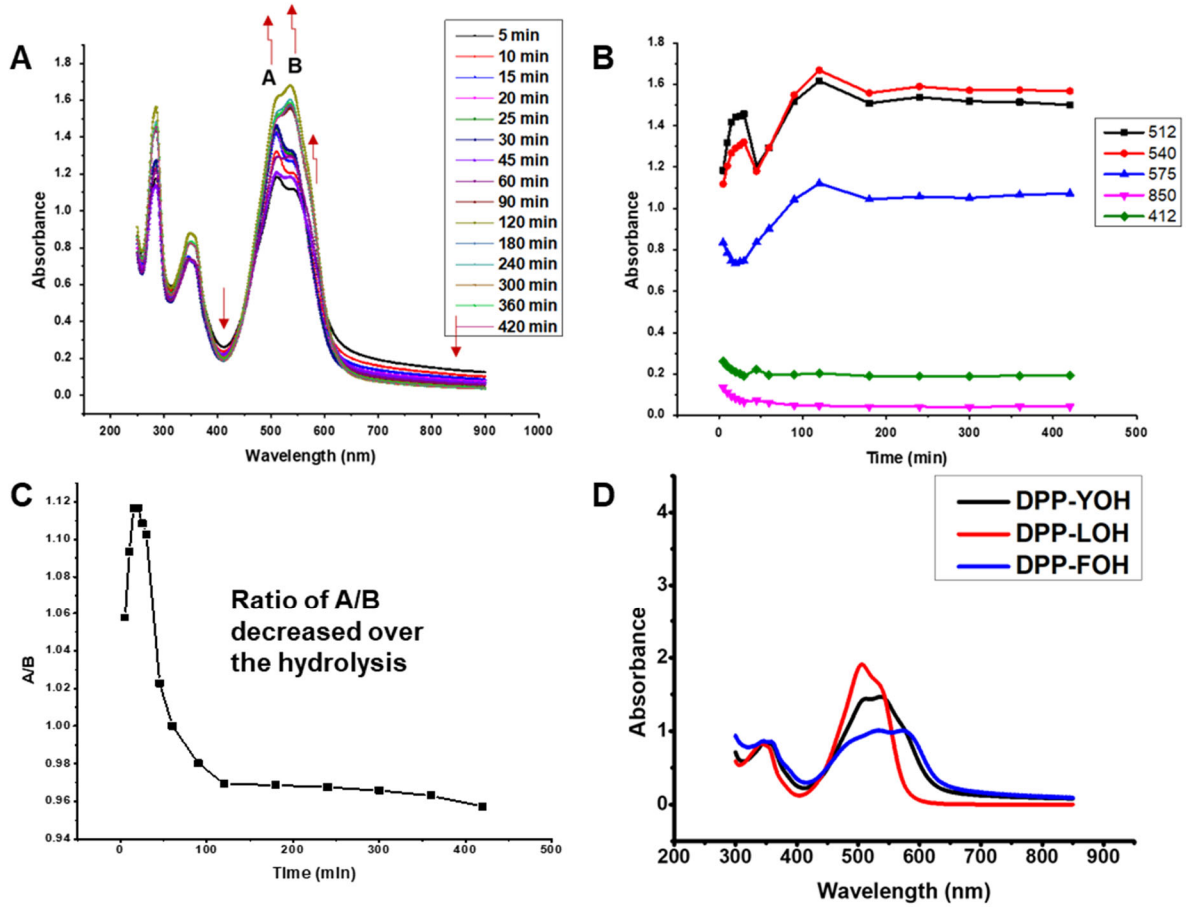

Figure S21. A) UV-Vis monitoring of enzymatic hydrolysis of **1Y** at 10 mM in phosphate buffer. B) Absorbance monitoring at different wavelengths during the hydrolysis of **1Y** at 10 mM in phosphate buffer. C) Change in the ratio of A/B during the hydrolysis of **1Y** at 10 mM in phosphate buffer. D) A) UV-Vis spectra of **3Y**, **3L** and **3F** at 10 mM in phosphate buffer.

8. Fluorescence spectroscopy

30 µl of reaction mixtures for the conversion of DPP-$(XOMe)_2$ to DPP-$(ROH)_2$ (10 mM in 100 mM phosphate buffer with 1 mg mL^{-1} α-chymotrypsin) at different time points were pipetted into a 0.1 mm demountable quartz cuvette and spectra were measured on a Jasco FP-8500 spectrofluorometer at a scanning speed of 200 nm min^{-1}. DPP samples were excited at 450 nm and were recorded between 460-800 nm using a bandwidth of 5 nm with a medium response and 1 nm data pitch.

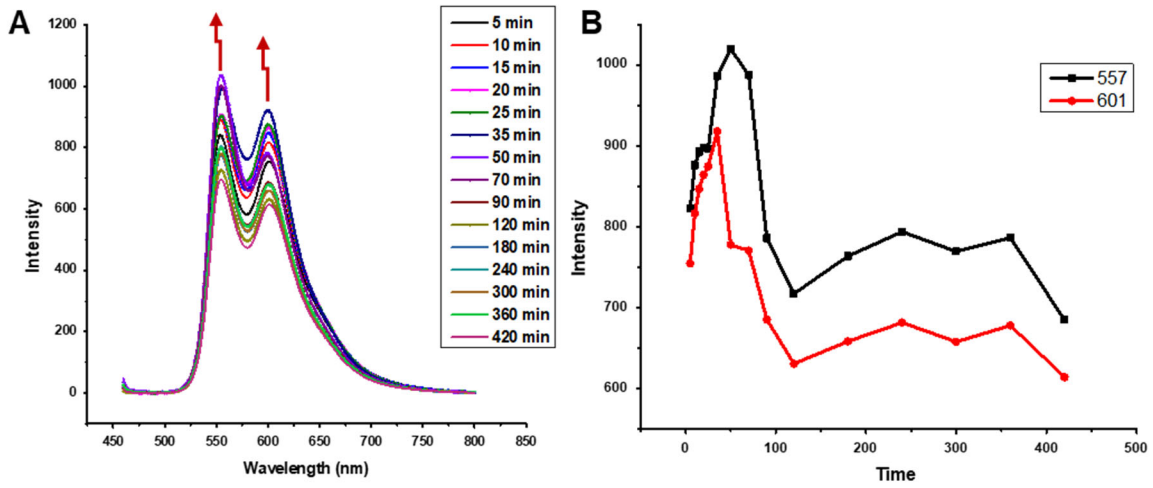

Figure S22. A) Monitoring of the enzymatic hydrolysis of **1Y** by Fluorescence. B) Fluorescence changes at different wavelengths of **1Y** during hydrolysis (Conc. 10 mM in phosphate buffer, λ_{ex}= 450 nm).

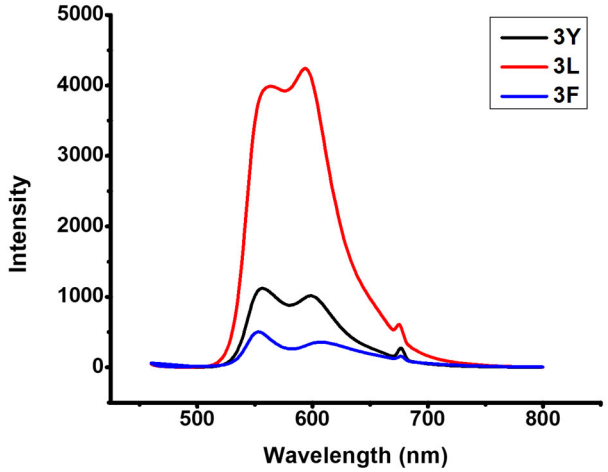

Figure S23. A) Fluorescence spectra of **3Y**, **3L** and **3F** at 10 mM in phosphate buffer (λ_{ex}= 450 nm).

9. Quantification of singlet oxygen generation

$^1O_2$ quantum yields were calculated following a previously reported approach.[2, 3] In brief air saturated DMSO was obtained by bubbling air into the solution for 15 min. To maintain the initial absorbance of DPBF and DPP-$(XOH)_2$ to about 0.1, a solution of 10^{-5} M of each were prepared and mixed in 1:1 ratio to minimize the possibility of $^1O_2$ quenching by the dyes. These solutions were then saturated with air for 5 min. The photooxidation of DPBF was monitored for 10 min. These mixtures were then excited (at different wavelengths depending on the λ_{ex} of each photocatalysts) for 2 min in a fluorimeter (Shimadzu, RF-5301pc) and absorbance were taken

(Shimadzu, UV-1800) immediately after excitation. This process was then repeated 5 more times. The decrease in absorbance at 418 nm due to photooxidation of DPBF by $^1O_2$ was then compared with MB to calculate $^1O_2$ yield. The spectra are shown in Figure S22. The quantum yields (Φ_Δ^{DPP}) of $^1O_2$ generation were calculated by a relative method using the Φ_Δ^{MB} of the photosensitizer to methylene blue (MB) (Φ_Δ, MB = 0.52) as the reference. Φ_Δ were calculated according to the following equation:

$$\Phi_\Delta^{DPP} = \Phi_\Delta^{MB} \frac{m^{DPP} F^{MB}}{m^{MB} F^{DPP}}$$

The superscript 'DPP' designates DPP derivatives, *m* is the slope of the plot DPBF (at 418 nm) vs. irradiation time, and F is the absorption correction factor, which is given by $F = 1\text{-}10^{-OD}$ (OD at the irradiation wavelength).

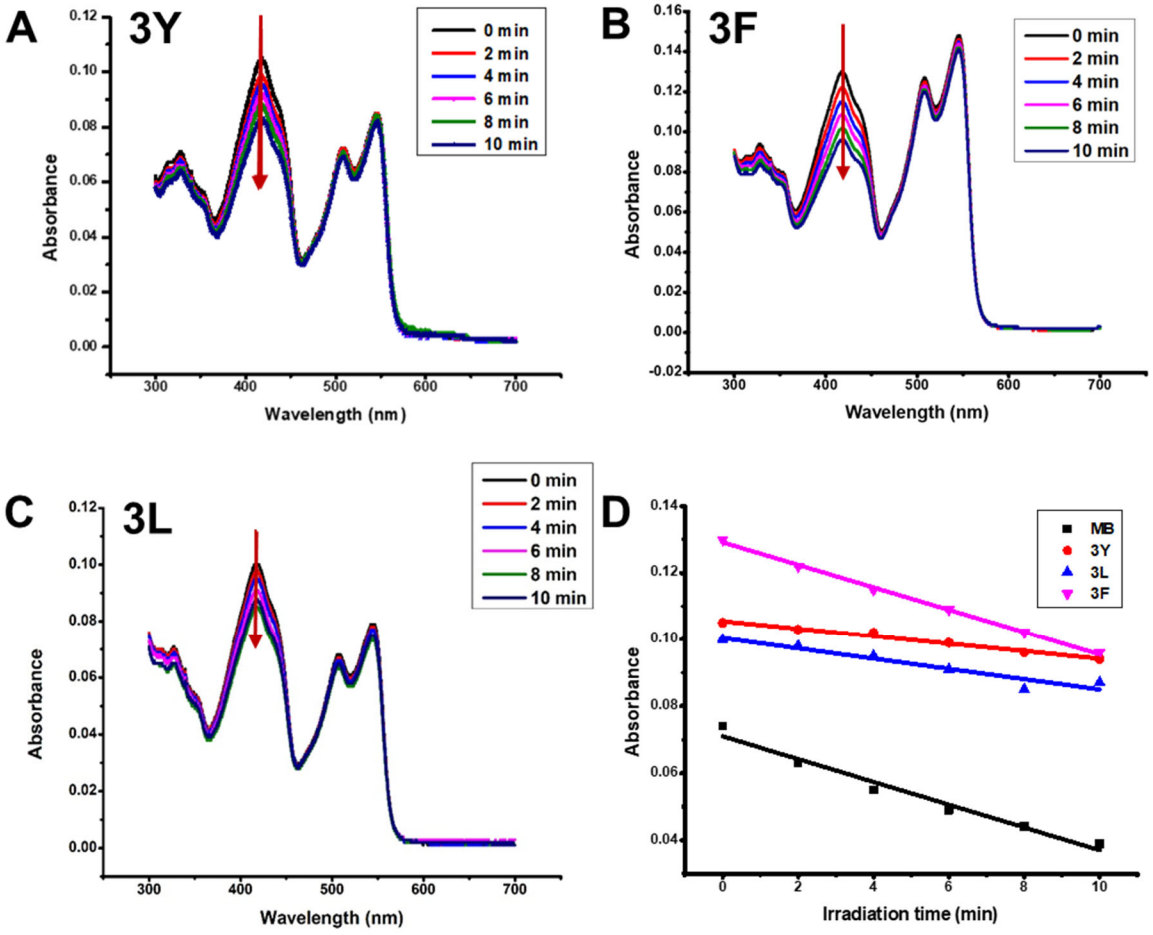

Figure S24. A) Changes in the absorption spectrum of DPBF upon irradiation (λ_{ex}= 535 nm) in the presence of **3Y** (recorded at 2 min intervals). B) Changes in the absorption spectrum of DPBF upon irradiation (λ_{ex}= 535 nm) in the presence of **3F** (recorded at 2 min intervals). C) Changes in the absorption spectrum of DPBF upon irradiation (λ_{ex}= 534 nm) in the presence of **3L** (recorded at 2 min intervals). D) Plot of the absorbance of DPBF at 418 nm *vs* irradiation time in the presence of DPP-$(XOH)_2$ against methylene blue as the standard.

10. Rheometry

Rheological properties were measured with an Anton Paar MCR 302 rheometer with temperature controlled at 25 ºC using a sand blasted geometry. The samples were prepared using a mold and 4 day-old samples were transferred onto the stage before measurements. First amplitude sweeps were performed at a constant frequency of 1 Hz from sheer strain 0.01-1% to ensure the measurements to be taken in viscoelastic regime. The frequency sweep was done to measure *G'* and *G"* at constant strain (0.4%) in the frequency range of 0.1-100 Hz.

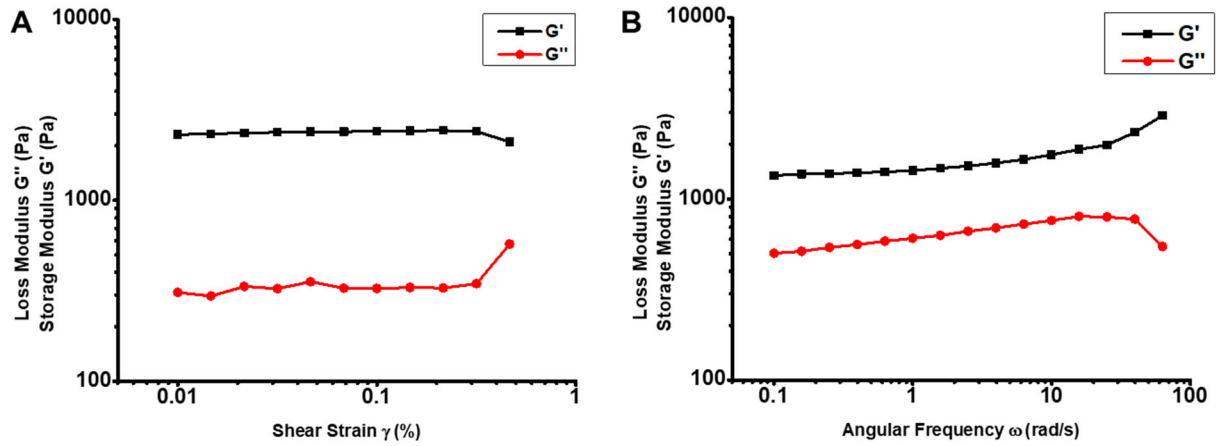

Figure S25. Storage (G') and loss moduli (G") of hydrogel **3Y** in amplitude sweep (**A**) and frequency sweep (**B**) at 10 mM.

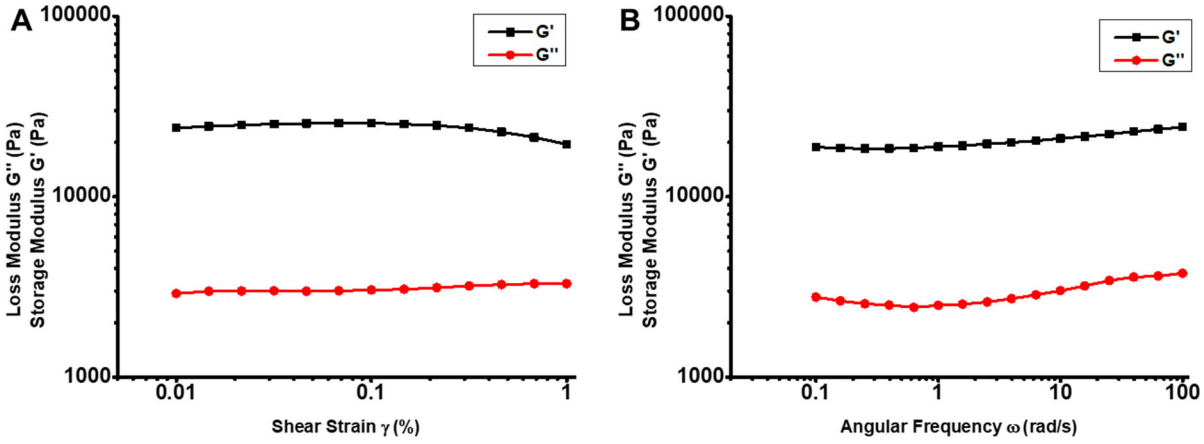

Figure S26. Storage (G') and loss moduli (G") of hydrogel **3F** in amplitude sweep (**A**) and frequency sweep (**B**) at 10 mM.

11. Characterization of the products of photooxidation

Thioanisole and cyclohexyl methyl sulfide were added to a solution of all catalysts (1.0 mL phosphate buffer of desired concentrations) maintaining 0.4 mM of the final concentration in the hydrogels, right after enzymatic hydrolysis of corresponding DPP-$(XOMe)_2$ without further purification, and stirred under positive pressure of air for 48 h. A white halogen light (150 W Fiber Optic Dual Gooseneck Microscope Illuminator), connected with optical fiber was used for photooxidation of thioanisole at rt**.** After 24 h, TLC (1:1 ethyl acetate/n-hexane) indicated the absence of starting material.

The crude reaction mixture for the sulfoxidation of thioanisole was washed in separatory funnel with H_2O (100 mL). The organic layer was collected and the aqueous phase was washed one more time with 100 mL CH_2Cl_2. The organic layer was collected and the aqueous phase was washed one more time with 100 mL of CH_2Cl_2. All organic layers were combined, dried with $MgSO_4$ and solvent was removed under reduced pressure. The product was then purified by column chromatography (SiO_2 1:99 EtOAc:CH_2Cl_2) to provide a colorless liquid. NMR matched with the reported compound[4] that was prepared following a different route.

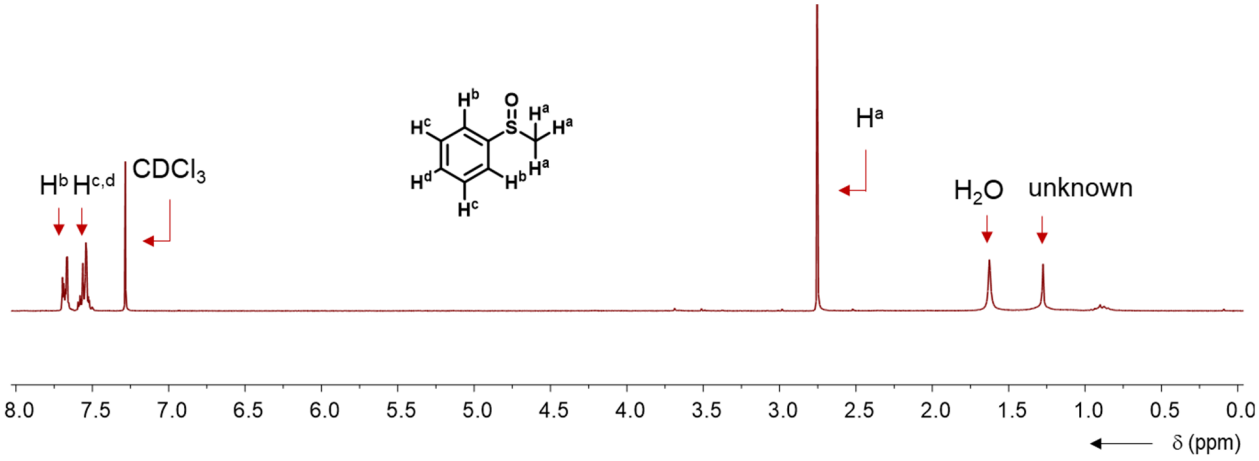

Figure S27. ^{1}H NMR of methyl phenyl sulfoxide (300 MHz, 25 °C) in $CDCl_3$.

In case of the sulfoxidation of cyclohexyl methyl sulfide, the product was directly extracted with 1.5 mL of $CDCl_3$. Organic layer was then dried using $MgSO_4$ before recording NMR. NMR matched with the reported compound[5] that was prepared following a different route.

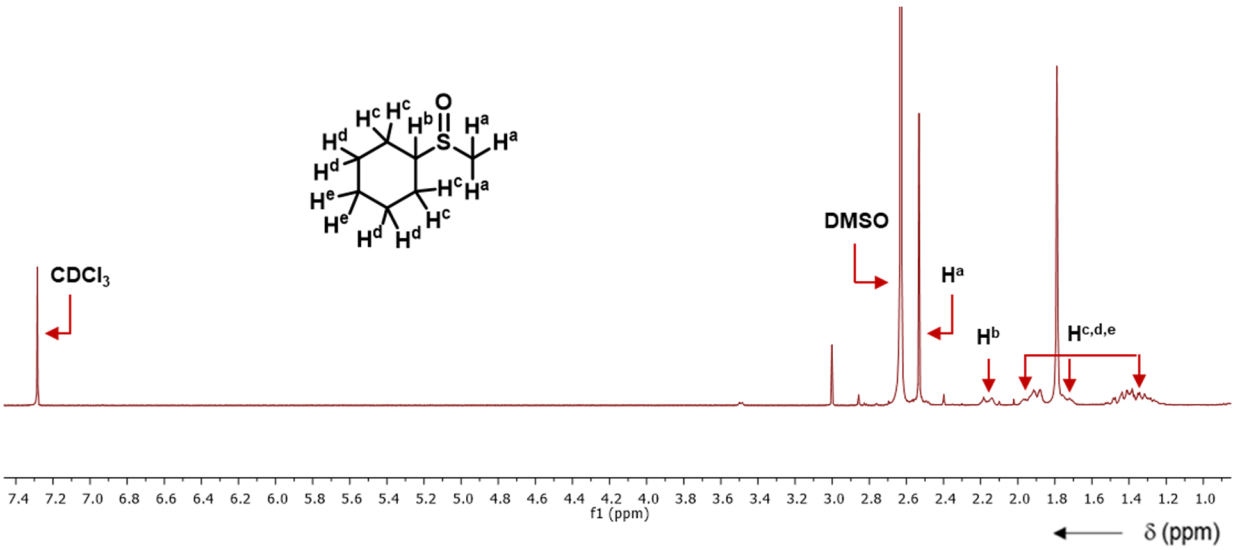

Figure S28. ^{1}H NMR of (Methylsulfinyl)cyclohexane (300 MHz, 25 ^{o}C) in $CDCl_3$.

Yield from the photooxidation of thioanisole and cyclohexyl methyl sulfide were calculated from HPLC, performed using a Daicel Chemical Industries, LTD 800 6-Chiral OD column. For the HPLC sample, 10 µl of the reaction mixture (with catalysts) were diluted to 0.5 ml of with MeCN. Vials with reaction mixtures were sonicated and vortexed for 3 min first before sampling. The eluting solvent system had a linear gradient of 3% (v/v) MeOH in H_2O (with 0.1% IPA) for 18 min. Chromatograms were monitored at 245 nm and the relative areas under the peaks were used to identify the percentage product conversion.

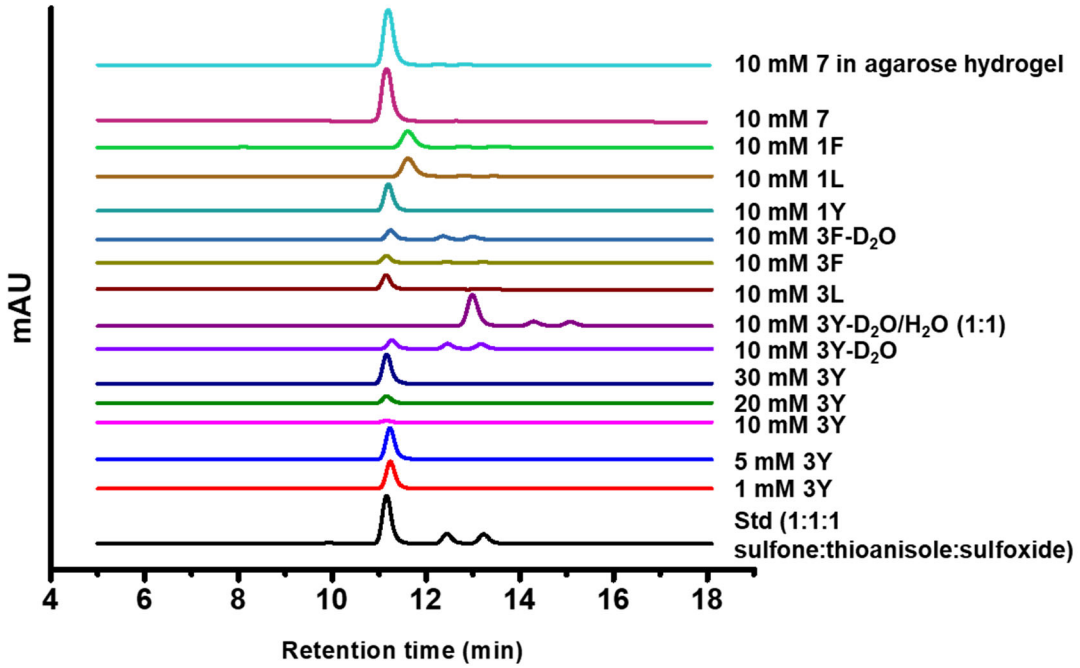

Figure S29. HPLC data for the photocatalytic sulfoxidation of thioanisole.

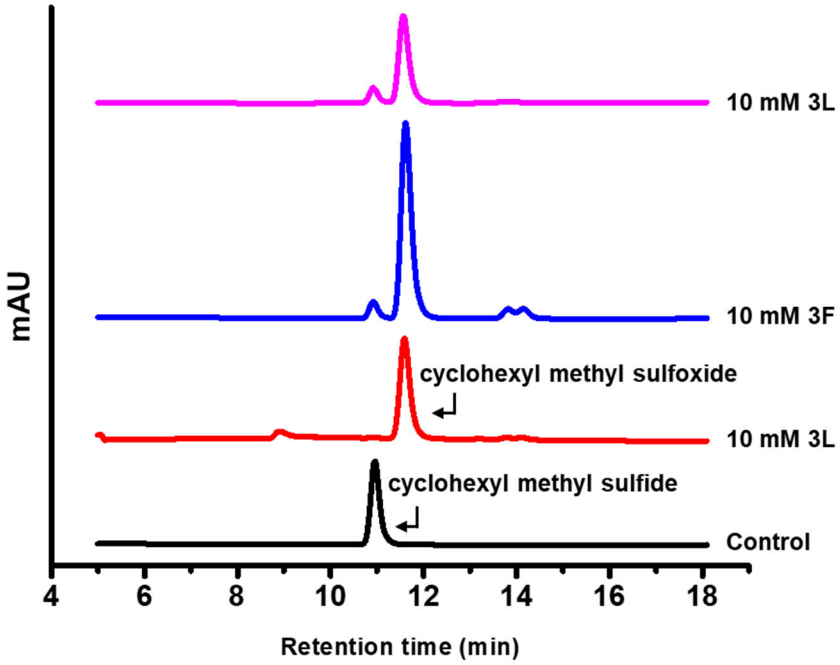

Figure S30. HPLC data for the photocatalytic sulfoxidation of cyclohexyl methyl sulfide.

12. References

1. E. R. Draper, B. Dietrich and D. J. Adams, *Chem. Commun.*, 2017, **53**, 1864-1867.
2. N. Adarsh, R. R. Avirah and D. Ramaiah, *Org. Lett.*, 2010, **12**, 5720-5723.
3. W. Li, L. Li, H. Xiao, R. Qi, Y. Huang, Z. Xie, X. Jing and H. Zhang, *RSC Advances*, 2013, **3**, 13417-13421.
4. N. D. Gillitt, J. Domingos and C. A. Bunton, *J. Phys. Org. Chem.*, 2003, **16**, 603-607.
5. J. Šturala, S. Boháčová, J. Chudoba, R. Metelková and R. Cibulka, *J. Org. Chem.* 2015, **80**, 2676-2699.